2018
International Symposium on Power Electronics,
Electrical Drives, Automation and Motion

Synchronous Reluctance Motor: Design, Optimization and Validation

M. Tursini, M. Villani, G. Fabri, A. Credo, F. Parasiliti
Dep. of Industrial and Information Eng. and Economics,
University of L'Aquila,
L'Aquila, Italy
marco.villani@univaq.it

A. Abdelli
Dept. Mechatronics,
IFP Energies Nouvelles,
Rueil-Malmaison F-92852, France
abdenour.abdelli@ifpen.fr

***Abstract*—The growing demand of high-performance motors requires the definition of more accurate design procedures. The only possibility to obtain such kind of results is to combine Finite Element programs with optimization procedures.**

For this reason, a multi-objective optimization algorithm has been developed, and it has been used to design a Synchronous Reluctance Motor with flux barriers rotor, starting from the stator core of a commercial three-phase induction motor of equivalent size. Based on the optimization results, a prototype has been built and tested.

Keywords— Flux barriers, Motor design, synchronous motors, reluctance motors, finite element analysis, optimization, multi-objective, motor tests, Rare Earth Free.

I. Introduction

The interest in using Synchronous Reluctance Motors (SyncRel) in different application fields is growing nowadays. SyncRel presents interesting advantages such as the low inertia, the high power-to-weight ratio, the good acceleration performance, the flux weakening operation, the low material costs and the easy of manufacturing [1].

Moreover, the SyncRel is a rare earth free machine and in times when the availability of rare earth is unsure [2] it is considered a promising motor technology for mass production products such as the motors for Electric Vehicles applications [3].

To this extent, SyncRel must feature very high salience ratio *Ld/Lq* obtained with multi flux barrier structure to achieve the required torque and power density.

The accurate design of the SyncRel is challenging because of its highly saturated operating conditions and its salient structure. It follows that the optimization of the motor geometry is difficult in particular in rotor configurations with a high number of flux barriers.

In this context, the authors developed an analytical procedure, by Finite Element (FE) model, that allows finding the "preliminary design" of the SyncRel [4]. Nevertheless, in order to obtain a more effective design, a multi-objective optimization algorithm is needed, for the design refinement.

The paper presents the design of a 4 poles, 20 Nm, 400 V, 50 Hz Synchronous Reluctance Motor with four flux-barriers.

For the sake of validation and tests of the design and optimization strategies for the SyncRel, a commercial TEFC three-phase induction motor of equivalent size (3kW, 4 poles, 400V, 50 Hz) has been considered as reference. For rapid prototyping the same stator core and housing have been used. The experimental results are presented and discussed at the end of this paper.

II. Preliminary Design

The preliminary design of the SyncRel has been carried out by a sizing procedure that allows determining all the geometrical data by adopting simplified relationships between geometrical and physical motor data in order to meet the motor specifications.

The motor performance calculation indicates the process of machine performance prediction, starting from geometry, material data and supply conditions. A detailed analysis is commonly performed to take into account the saturation and cross-magnetization effects.

The procedure begins with the assignment of the following input data:

- the output torque;
- the phase voltage and current density;
- the frequency, the number of poles and stator slots;
- the number of rotor flux barriers;
- the air-gap flux density;
- the flux densities in the stator tooth and stator yoke;
- the minimum power factor;
- the maximum slot filling factor.

The output of the sizing procedure consists in the geometric dimensions of the stator core and of the rotor shape, and the stator winding. These data allow calculating the motor performance i.e. the axis fluxes, the magnetic potential differences, the flux densities, the axis currents, the power factor, and the torque. A detailed description of the sizing procedure is given in [5].

The sizing of the rotor is not easy to carry out due to the presence of the flux barriers whose number and dimensions directly affect the *saliency ratio*, that is the ratio between *d* and *q-axis* inductances. For this reason, the authors have introduced several relationships among the rotor dimensions (Fig.1) and the rotor diameter (D_r), by means of suitable coefficients (k_i).

978-1-5386-4941-1/18/$31.00 ©2018 IEEE

These relations and the coefficients have been refined and tested analyzing several SyncRels, of different size, by the Finite Element Analysis and represent a guideline for the designer and should orient him towards the search for suitable solution: for a rotor with two flux barriers, they are reported in (1).

Moreover, the presented approach is fundamental for the next optimization steps, where the coefficients k_i are imposed in the input data, and these values define a range within each variable should vary according to the imposed values on D_r. The sizing process starts considering a preliminary design realized by considering the average value of each variable. The design refinement is then reached by the optimization algorithm (Section B).

$$\begin{array}{ll} k_1 D_r \le fb1 \le k_2 D_r; & k_3 D_r \le a1d \le k_4 D_r \\ k_5 D_r \le b1 \le k_6 D_r; & k_7 D_r \le b2 \le k_8 D_r \\ fb_2 \le k_9 fb_1 & fb_3 \le k_{10} D_r \end{array} \quad (1)$$

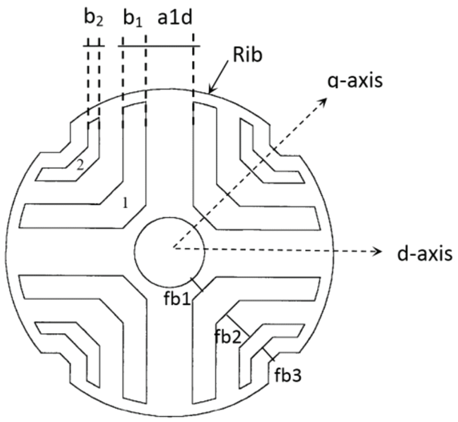

Fig. 1. Example of a two barrier rotor with related dimensional variables.

The number of flux barriers (N_{barr}) has been calculated according to the number of stator slots (N_{slot}) and the number of poles (N_{pole}) following relationship:

$$(N_{barr})_{tot} = N_{pole} K_i \qquad K_i \ne \frac{N_{Slot}}{N_{pole}} \quad (2)$$

It is important to underline that increasing the amount of flux–barriers, the torque tends to increase whereas the torque ripple decreases.

Considering the aim to design and realize a SyncRel, starting from a commercial three-phase induction motor of equivalent size (3kW, 4 poles, 400V, 50 Hz), the same stator core and housing has been adopted, substituting the squirrel cage rotor with a flux-barriers one. The sizing procedure has concerned only the design of the rotor shape and stator winding. The number and width of flux barriers were calculated according to the number of stator slots. Since the chosen stator core presents *36* slots, a suitable choice of the number of flux barriers is four (Fig.2). Moreover, the motor has been designed with reference to the operating point at maximum power factor [1].

TABLE I. presents the performance and the main geometric dimensions of the preliminary design.

This preliminary design has been then deeply investigated by mean of an accurate parametric bi-dimensional FE model developed by a commercial software including the mechanical equation with usual coefficient for the computation of windage and friction losses. The parametric model allows modifying any geometric dimensions of stator and rotor shape, the rotor position and the currents.

The FE analysis results of the preliminary design, have been compared with the sizing procedure ones (TABLE II. In both analyses, the same axis currents have been imposed. Moreover, the FE magnetostatic analyses have allowed to evaluating the SyncRel torque behavior for different rotor positions (in this case the inductance values depend on the rotor position only) and then to calculate the torque ripple, (about 14% for the no-skewed rotor).

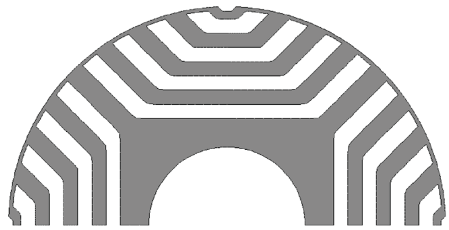
Fig. 2. View of the rotor with four flux barriers output of the preliminary design procedure (half of the rotor).

TABLE I.
MEANINGFUL DATA AND PERFORMANCE OF THE PRELIMINARY DESIGN.

Data		Value
Number of poles		4
Stack length	(mm)	130
Outside stator diameter	(mm)	152
Inner stator diameter	(mm)	90
Stator slots		36
Number of flux barriers per pole		4
Number of turns per phase		198
Phase voltage (RMS)	(V)	198
Speed	(rpm)	1500
Phase current (RMS)	(A)	7.7
Id	(A)	3.7
Iq	(A)	10.2
Torque	(Nm	20.0
Power factor		0.76
Saliency ratio		7.84

TABLE II.
COMPARISON BETWEEN SIZING PROCEDURE (SP) AND FEA RESULTS (PRELIMINARY DESIGN).

Data		SP	FEA
Speed	(rpm)	1500	
Rated torque	(Nm)	20.0	19.6
Phase current (RMS)	(A)	7.7	7.7
Id	(A)	3.7	3.7
Iq	(A)	10.2	10.2
Phase voltage	(V)	198	200
Power factor		0.76	0.74
Flux density in the tooth	(T)	1.47	1.53
Flux density in the yoke	(T)	1.23	1.28

III. Design Refinement by Optimisation Algorithm

To achieve high-performance SyncRel the geometry of the flux barriers has to be carefully designed, and especially with more than two barriers the complexity of the optimization problem requires adoption of automatic optimization procedures.

In this case, the geometric parameters become the independent variables of an optimization problem while the performances of the motor are objective functions or constraints of the optimization problem.

The optimization procedure can use the FE analysis to iteratively compute the performance of the motor and then update the set of geometry parameters in the attempt to identify an "optimal" design by making a trade-off between the different parameters and constraints of the machine.

This approach requires the use of suitable optimization algorithms, namely the use of algorithms that can cope with minimization problems which present the following distinguishing difficulties:

a) the particular nonlinear structure of the objective function (and, possibly, of the constraints) produces the existence of different local minimum points, besides the global ones;

b) the physical nature of the constraints implies that the Finite Element based objective function cannot be defined or computed outside the "feasible region" and that the region of the feasible motor parameters is "relatively large";

c) the use of the Finite Element Analysis has the consequence that the explicit mathematical representation of the objective function and of some of the constraints are not available. It follows that the evaluations of the objective function and those constraints can be expensive and affected by numerical errors.

For this work, a global minimization algorithm able to take features *a*), *b*) and *c*) into account in finding the optimal design of Synchronous Reluctance motor has been carried out. To this aim, we have defined a new global optimization algorithm belonging to the class of Controlled Random Search (CRS) Price algorithm firstly proposed in [6]. The adoption of this class of algorithms appeared very promising in finding the optimal design of electric motors.

CRS Price algorithms have been proven to be useful and effective in solving several global optimization problems deriving from real-world applications [7], [8]. Similarly, to other global optimization methods, CRS algorithms follow a strategy which combines a global search phase and a local search phase. The global search is used to locate the sub-regions "more promising" to contain a global minimizer; the local search is used for determining the global minimizer as soon as a "sufficiently small" neighborhood of this point has been located.

The basic idea of CRS methods is that of randomly generating an initial set of sample feasible points and iteratively updating this sample by substituting the worst point, in terms of objective function value, with a better one obtained by a local search. In this way the set of sample points should cluster more and more round the sub-regions which are more likely to contain a global minimizer. Therefore, these methods follow an approach which can be considered a compromise between a purely random search strategy and a clustering strategy derived by a deterministic local search.

Starting from the original method proposed by [6], several new CRS algorithms have been proposed [7], [8]. The modifications introduced in these algorithms have the common aim of exploring as much as the information on the minimization problem obtained during the iterates of the algorithm.

Recently, in [9] a new version of the CRS Price algorithm has been proposed and its affective computational behavior has been shown in solving optimization problems of a permanent magnet synchronous motor. In particular the numerical results reported in [9] have pointed out the efficiency of this CRS method in locating a global minimum in this class of electric motors design problems.

This algorithm has been interfaced with the FE analysis procedure and it has been used for the refinement of the SyncRel preliminary design presented in the previous Section.

The aim of optimization was to maximize the rated torque and power factor (referring to the base speed of 1500 rpm) and minimize the torque ripple. A good design should represent the right compromise among different objectives but the problem consists in searching this "compromise". The only tool able to solve this problem is represented by the Multi-objective approach [7, 9].

This approach allows us to investigate how each single-objective and multi-objective problem affect the results in terms of performance and independent variables and, above all, allows us to have a wide range of alternative designs among which the designer can choose a better solution.

The torque for the SyncRel in the rotor reference frame is:

$$T = \frac{3}{2} p \left(L_d - L_q\right) I_d I_q \tag{3}$$

and the power factor is:

$$pf_i = \frac{k_s - 1}{\sqrt{\left(k_s^2 \frac{1}{\sin^2 \varepsilon}\right) + \frac{1}{\cos^2 \varepsilon}}} \tag{4}$$

where L_d and L_q are, respectively, the direct and quadrature axis inductances, p is the number of pole pairs, I_d and I_q the direct and quadrature axis currents, k_s the saliency ratio (L_d/L_q) and ε the current angle between the space vector of the stator current (I_s) and the d-axis current.

The analytical expressions of (4) and (5), respect to the design variables, are not available, and their values have been provided by a Finite Element analysis of the motors.

The independent variables concerned the rotor only and particularly the dimensions of the flux barriers; moreover, two further variables have been introduced in order to vary the inclination of the flux barriers.

In addition, the following constraints have been considered: phase voltage, which is related to the maximum voltage of the inverter, power factor, flux densities in the stator teeth and yoke, specific losses in the slot, torque, torque ripple and slot fullness. Table III shows the imposed limit values on the constraints. For the SyncRel design optimization, several stator-rotor relative positions have been analyzed by FE model, and the performances correspond to the average values.

The optimization has concerned the no-skewed rotor since the skewing would have required high computation times for each call of the FE program.

About the reduction of the torque ripple is worth to notice that even if particular geometry solutions are adopted an effective optimization of the barriers design has always a strong impact on the torque ripple minimization [10].

The rotor shape of the optimized design is shown in Fig.3, while the performances of the new motor are presented in Table IV and they are compared with the preliminary design ones. Fig.4 shows the torque ripple for the preliminary and optimized design, the new rotor shape allows a significant reduction in the torque ripple, with satisfactory values of the torque and power factor.

TABLE III.
LIMIT VALUES ON THE CONSTRAINTS
(WITH REFERENCE TO THE BASE SPEED OF 1500 RPM).

Average flux density in the stator yoke	(T)	< 1.5
Average flux density in the stator tooth	(T)	< 1.8
Phase voltage	(V)	< 210
Power factor		> 0.70
Specific losses	(W/dm^2)	< 15
Torque	(Nm)	> 18
Torque ripple	%	< 10
Slot fullness		< 0.45

TABLE IV.
PERFORMANCE OF THE PRELIMINARY AND OPTIMIZED DESIGNS (BY FEA).

Data		Preliminary	Optimized
Speed	(rpm)	1500	
Rated torque	(Nm)	19.6	20.3
Phase current (rms)	(A)	7.7	7.7
Id	(A)	3.7	3.7
Iq	(A)	10.2	10.2
Phase voltage	(V)	200	203
Power factor		0.74	0.76
Flux density in the tooth	(T)	1.53	1.64
Flux density in the yoke	(T)	1.28	1.50
Torque ripple (no-skewed)	%	14	4.5

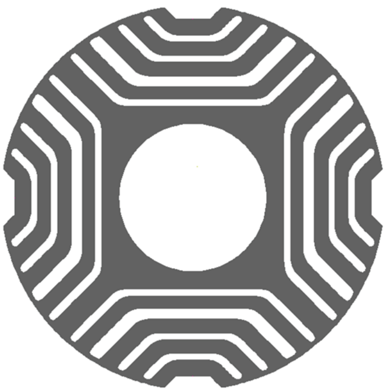

Fig. 3. Rotor shape of the optimized design.

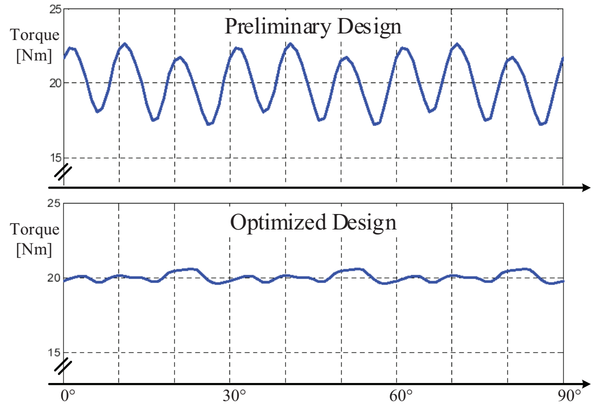

Fig. 4. Detail of the Torque and Torque ripple Vs mechanical position.

IV. EXPERIMENTAL TESTS AND RESULTS

Starting from the optimization results, a prototype of SyncRel has been built. Particularly, the rotor laminations have been realized by "laser cut" and assembled to make up the rotor core: a rotor skewing of one slot pitch has been chosen for a further reduction of the torque ripple.

The rotor laminations have been jammed by soldering along the rotor surface (on the external barrier); moreover, two shields in aluminum have been introduced on the shaft in order to press the rotor core. Figure 5 shows the rotor core and a view of the rotor lamination.

In order to verify its performance, the SyncRel motor has been tested through the experimental set-up shown in Fig.6. It includes a current vector controlled Voltage-Source (VS) inverter, with superimposed speed control loop, the SyncRel motor fed through a digital power meter (Yokogawa WT3000), and a brake. Phase current (I_s), voltage (V_s), active power (P_{in}), and power factor at the motor input terminals are measured by the digital power meter. Constant speed (ω_r) is assured by the speed control loop of the drive, while constant load torque (T_{out}) is imposed through the brake; thereafter constant output power (P_{out}) operation is achieved.

The drive vector control allows to impose (independently) the set point of the direct current component (i_d), while the speed regulator adjusts the set-point of the quadrature current component (i_q). With this scheme, the value of the (actual) quadrature current depends on the torque and the commanded direct current: hence, by changing the set-point of the direct current, one can test the performance of the SyncRel at constant torque and speed with different orientation of the current vector including a fine tuning of the Maximum Torque Per Ampere (MTPA) control strategy.

For the sake of accuracy in the experiments, the SyncRel motor has been equipped with a high resolution position encoder, giving 8192 pulses per revolution. The direct and quadrature currents, computed by the drive, are detected through the user interface of the drive, while the speed is measured directly on the brake. Other basic info of the drive system are as follows: Semikron IGBT power modules, rating 100Amps, 1200V, operated at 10kHz PWM frequency;

Spectrum Digital "ezDSP" control module, based on the TMS320C2812 Digital Signal Processor.

Several tests have been carried out on the SyncRel prototype, meaningful tests are reported in the following. About the torque ripple, it has not been directly measured but one can report that the prototype is extremely silent in all the tests. The motor efficiency is reported in Table V and VI at different rotor speed and the power factor at rated speed is reported in Table VII. Table VIII reports a comparison between the performances of the SyncRel and the original Induction Motor (IM) with copper rotor. The power density of the SyncRel is 3.5% better than the induction motor and the motor efficiency is also increased. Nevertheless, the current required by the SyncRel is 10% higher and it could affect the sizing and the efficiency of the converter.

All the results have been carried out MTPA control strategy and includes the measurements reported in comparison with the results obtained by the FE analysis. The measures are derived only from the fundamental components of stator currents and stator voltages.

Figure 7 reports the trend of the torque versus the current angle with the experimentally detected MTPA control strategy. Each torque values requires a precise current angle to guarantee the maximum performance of the motor. Also the speed influences the current angle due to the different performance of the electrical steel at different frequencies.

Figure 8 reports the torque constant versus the output torque of the motor. One can notice how the torque constant is not affected by the speed variations except in the point 20Nm, 1500rpm where the motor works in voltage limitation.

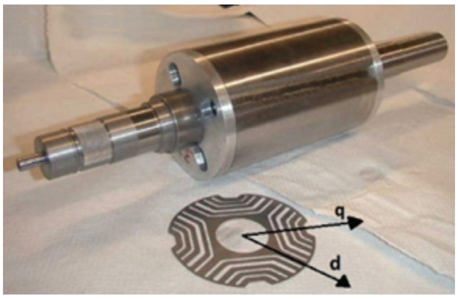

Fig. 5. Rotor core of the optimized SyncRel.

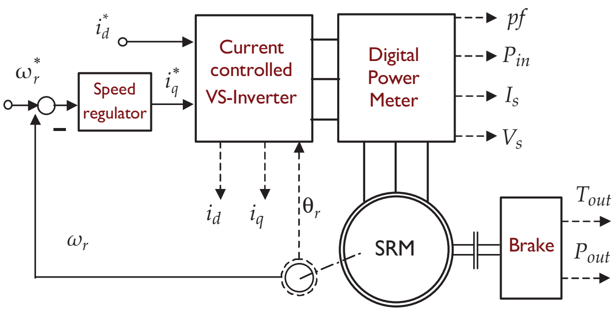

Fig. 6. SyncRel drive and measurement set-up.

TABLE V. MOTOR EFFICIENCY @1000RPM.

	Efficiency @ 1000 rpm		Error %
Torque [Nm]	**FE Analysis**	**Experimental**	
4	0.868	0.876	0.91%
6	0.873	0.877	0.46%
8	0.874	0.873	-0.11%
10	0.871	0.870	-0.11%
15	0.856	0.841	-1.78%
20	0.828	0.843	1.78%

TABLE VI. MOTOR EFFICIENCY @1500RPM.

	Efficiency @ 1500 rpm		Error %
Torque [Nm]	**FE Analysis**	**Experimental**	
4	0.889	0.894	0.56%
6	0.895	0.897	0.22%
8	0.900	0.898	-0.22%
10	0.900	0.895	-0.56%
15	0.894	0.881	-1.48%
20	0.871	0.870	-0.11%

TABLE VII. MOTOR POWER FACTOR @1500 RPM.

	Power Factor @ 1500 rpm		Error %
Torque [Nm]	**FE Analysis**	**Experimental**	
4	0.554	0.597	7.20%
6	0.581	0.597	2.68%
8	0.616	0.621	0.81%
10	0.636	0.641	0.78%
15	0.695	0.697	0.29%
20	0.734	0.728	-0.82%

TABLE VIII. COMPARISON BETWEEN SYNCREL AND IM.

Data		SyncRel	IM
Weight	(kg)	22.2	23.0
Efficiency @20Nm, 1500 rpm	(-)	0.87	0.84
Phase Current @ 20Nm, 1500 rpm	(A)	7.54	6.86
Power Factor	(-)	0.73	0.81

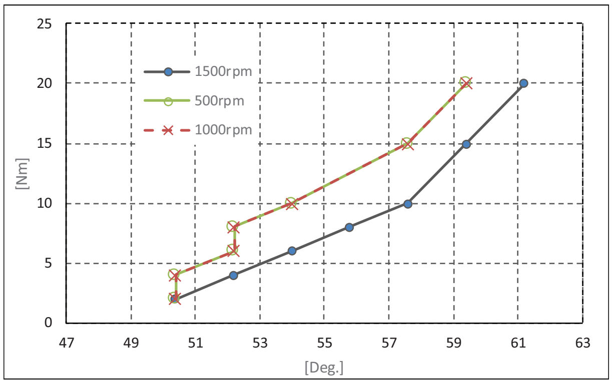

Fig. 7. Current angle for MTPA control strategy versus output torque at different speed values.

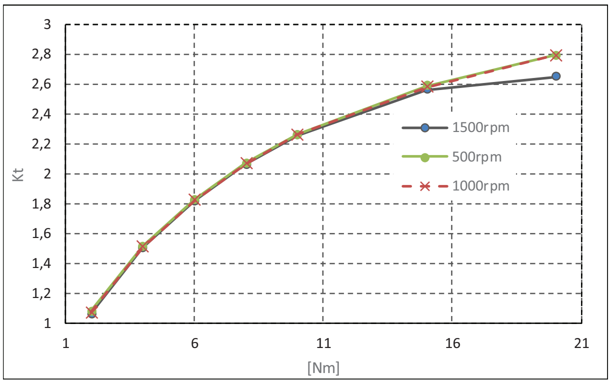

Fig. 8. Torque versus Torque-current Ratio (Torque Constant k_t) at different speed.

V. Conclusion

The 2D Finite Element analysis together with an optimisation algorithm has been used for the design of the SyncRel with rotor flux barriers. The design of the rotor has been customized to realize a SyncRel starting from the stator core of a commercial three-phase induction motor of equivalent size with advantages in the validation of the design and optimization strategies. From the optimization results, a prototype of SyncRel has been built and tested.

The obtained results are satisfactory and point out the effectiveness of the design approach since they represent a good compromise among the proposed goals.

The goodness of the results achieved with the proposed algorithm shows that combining the FE analysis with a suitable optimization strategy is an effective and powerful tool for the design optimization of electric motors.

Acknowledgment

This project has received funding from the European Union's Horizon 2020 research and innovation programme under the Grant Agreement No (770143)

References

[1] Boldea, Reluctance synchronous machines and drives. Oxford: Clarendon Press, 1996.

[2] E. Alonso, A. Sherman, T. Wallington, M. Everson, F. Field, R. Roth and R. Kirchain, "Evaluating Rare Earth Element Availability: A Case with Revolutionary Demand from Clean Technologies", *Environmental Science & Technology*, vol. 46, no. 6, pp. 3406-3414, 2012.

[3] J. Widmer, R. Martin and M. Kimiabeigi, "Electric vehicle traction motors without rare earth magnets", *Sustainable Materials and Technologies*, vol. 3, pp. 7-13, 2015.

[4] F. Parasiliti and M. Villani, "Synchronous reluctance motors design and performance prediction using an analytical procedure",, *Electrical Engineering and Electromagnetics*, WIT Press, 2003, ISBN- 1-85312-981-X, pp. 147-156.

[5] F. Parasiliti and M. Villani, "Magnetic analysis of flux barriers Synchronous Reluctance Motors", *2008 18th International Conference on Electrical Machines*, 2008.

[6] W.L. Price, A controlled random search procedure for global optimization, In L.C.W. Dixon and G.P. Szego, editors, Towards Global Optimization 2, North-Holland, Amsterdam, 1978.

[7] W. L. Price, Global optimization by controlled random search, *Journal of Optimization Theory and Applications*, 40 (1983), 333-348.

[8] P. Brachetti, M. De Felice Ciccoli, G. Di Pillo and S. Lucidi, Journal of Global Optimization, vol. 10, no. 2, pp. 165-184, 1997.

[9] F. Parasiliti, M. Villani, S. Lucidi and F. Rinaldi, "Finite-Element-Based Multiobjective Design Optimization Procedure of Interior Permanent Magnet Synchronous Motors for Wide Constant-Power Region Operation", *IEEE Transactions on Industrial Electronics*, vol. 59, no. 6, pp. 2503-2514, 2012.

[10] B. Gaussens, J. Boisson, A. Abdelli, L. Favre and D. Bettoni, "Torque ripple mitigation of PM-assisted synchronous reluctance machine : Design and optimization", *2017 20th International Conference on Electrical Machines and Systems (ICEMS)*, 2017.